

# Development of Faraday-cup-based Fast Ion Loss Detector in Wendelstein 7-X

K. Ogawa<sup>1,2</sup>, M. Isobe<sup>1,2</sup>, M. Osakabe<sup>1,2</sup>, S. A. Bozhakov<sup>3</sup>, S. Äkäslompolo<sup>3</sup>, C. Killer<sup>3</sup>,  
C. Biedermann<sup>3</sup>, R. C. Wolf<sup>3</sup>, and the W7-X team

<sup>1</sup> National Institute for Fusion Science, National Institutes of Natural Sciences, Toki, Japan

<sup>2</sup> SOKENDAI (The Graduate University for Advanced Studies), Toki, Japan

<sup>3</sup> Max-Planck-Institute for Plasma Physics, Greifswald, Germany

Study of fast-ion losses due to magnetic field ripples and fast-ion-driven magnetohydrodynamic (MHD) modes is an important research regarding fusion-born alpha losses [1]. In order to understand fast-ion losses in Wendelstein 7-X (W7-X) plasmas, installation of fast-ion loss diagnostic is planned [2]. For the upcoming OP1.2b campaign in 2018, a prototype Faraday-cup-based fast-ion loss detector (FILD) has been designed as a joint cooperative project between National Institute for Fusion Science (NIFS) and Max Planck Institute for Plasma Physics. The Faraday-cup-based FILD, which is relatively cost-effective in construction compared with a scintillator-based FILD, has been installed to measure the fast ion loss flux in the Compact Helical System (CHS) [3, 4], the National Spherical Torus eXperiment (NSTX) [5], the Joint European Torus (JET) [6, 7], the Doublet III-D (DIII-D) [8], and the Heliotron-J [9, 10]. The FILD is capable of measuring the flux, the pitch angle ( $\chi$ ), and the energy ( $E$ ) of escaping fast ions simultaneously, thus providing a clear understanding of fast-ion losses induced by MHD modes and non-axisymmetric magnetic field ripples. An increase of co-going fast-ion losses due to energetic particle modes (EPM) and toroidal Alfvén eigenmodes (TAE) was reported in CHS [4].

The NIFS Lorentz orbit code (LORBIT) [11] has been used to find a position suitable to detect escaping fast ions in the high-mirror configuration in W7-X. The LORBIT code is based on the equation of motion of a charged particle. Figure 1 shows the FILD

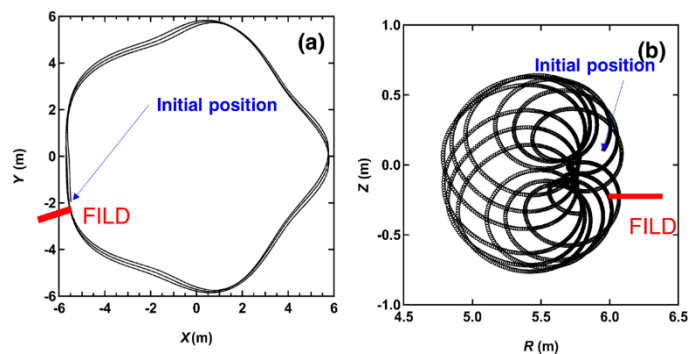


Fig. 1 Typical beam ion orbit and FILD position in W7-X. (a) Overhead view and (b) projected onto the  $(R, Z)$  plane.

positions together with a typical beam ion orbit as seen from the top and as projected into the  $(R, Z)$  plane. Here, the start position of the orbit is  $(x, y, z) = (-5.48 \text{ m}, -1.96 \text{ m}, -0.33 \text{ m})$ .  $E$  and  $\chi$  of the particle is 60 keV and -119 degrees, respectively at the initial position. In this calculation, we follow an orbit of  $10^6$  particles having  $E$  of 60 keV from the deposition position of neutral beams injected by beam ion sources #3, #4, #7 and #8 [12]. Here, the location of the FILD head is changed along the path of the movable Multi-Purpose Manipulator (MPM) [13] on which the FILD will be mounted in OP1.2b. The radius of the FILD head is set to be 50 mm. Figure 2 (a) and (b) shows the number of particles reaching the FILD in each position and its  $\chi$  distribution. The number of particles gradually increases from  $R$  of around 6.10 m. The heat flux distribution due to the beam ion evaluated by ASCOT codes which is a guiding center orbit following code with collisions [14] shows that the sufficient heat load comes to the FILD tips (Fig.2 (c)). The calculation results indicate that we can measure barely-passing ( $\chi$  of around -130 degrees and -60 degrees) and trapped ( $\chi$  of around -90 degrees) beam ions.

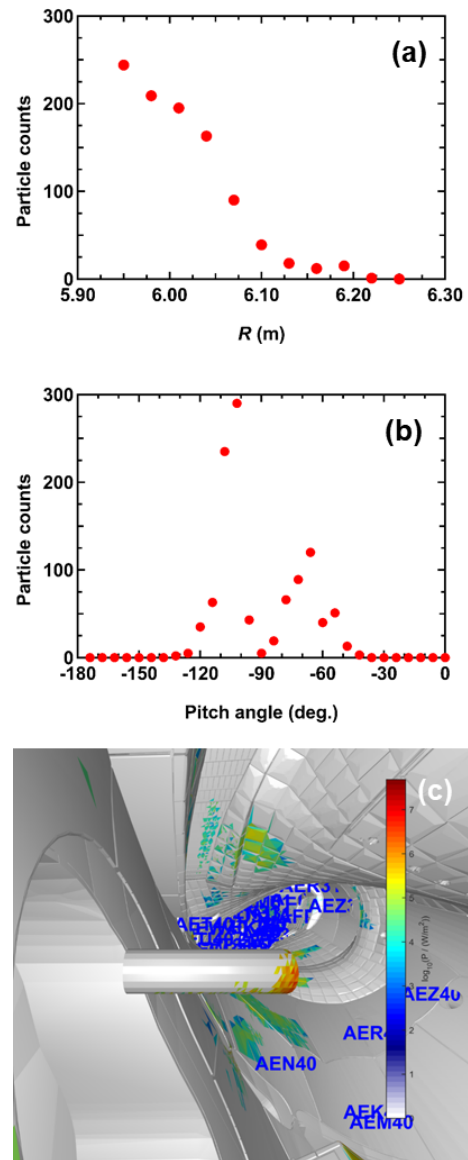


Fig. 2 (a) Radial distribution and (b) pitch angle distribution of particle counts detected by the FILD. (c) Distribution of heat flux due to beam ions to the FILD.

The detector is mainly composed of a molybdenum head and eight Faraday films. The molybdenum head has two apertures which restrict the orbit of energetic ions that can enter the probe. The Faraday films have a function of charge collectors. The detector is surrounded by the graphite cover in order to prevent the heat damage of the detector (Fig. 3). The size and the position of those apertures are decided using the grid calculation program [15].



Fig. 3 Prototype FILD

Faraday film is a thin film of aluminum vapor deposited onto one side of the quartz substrate. The thickness of the films is approximately 0.2  $\mu\text{m}$ . The layout of eight Faraday films is also decided by means of the grid calculation program. We made two patterns of layout called pattern (a) and (b) as shown in Fig. 4. These have two energy and four pitch angle ranges. The pattern A has relatively narrow energy range in low-energy side compared with the pattern B. Note that the minimum detection energy of the FILD is around 30 keV. Electrical current from each Faraday film will be carried to the low input impedance current amplifier (I-76, NF Corporation, conversion factor of  $10^6$  V/A and frequency bandwidth of up to 20 kHz) and an isolation amplifier (HIS-LV, DEWETRON, frequency bandwidth of up to 2 MHz).

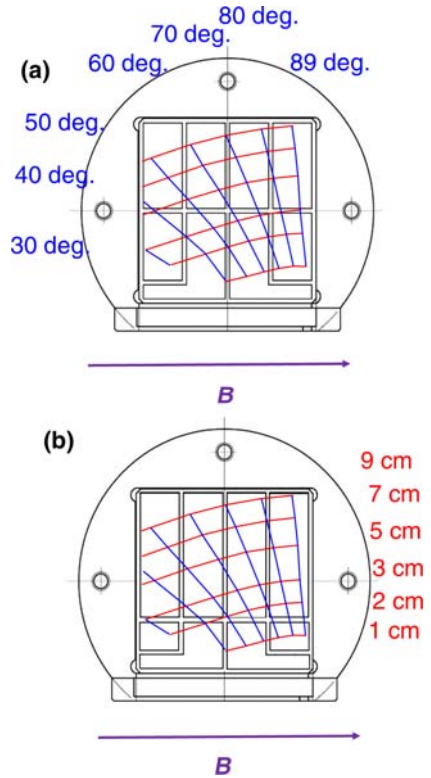


Fig. 4 The arrangement of Faraday film and the grid of the energy Larmor radius and the pitch angle.

The signal level of each Faraday film with pattern (a) is predicted using ASCOT codes. The response of the FILD is obtained based on the geometry of the apertures and the Faraday films. We launched  $10^6$  particles having various velocities from the first aperture and judged where the particle reaches. Here, proton energy of up to 200 keV is considered. The image map shown in Figure 5 indicates that the energetic ions having the energy of above 150 keV can reach the high-energy part of Faraday films #1 to #4, whereas from 30 to 200 keV the beam ions mainly reach the lower-energy part of Faraday films #5 to #8, as designed. We estimated the expected beam ion

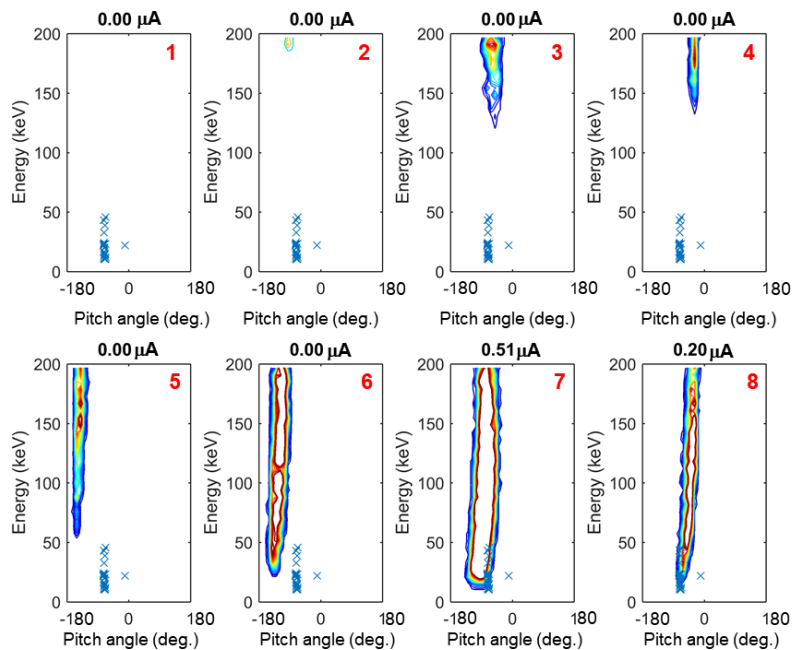


Fig. 5 Evaluation of the signal in each film for pattern (a) by ASCOT code.

current by comparing the FILD response and the  $E/\chi$  distribution of beam ions that reached to the FILD. Here,  $E/\chi$  distribution of beam ions is obtained by ASCOT code and shown by the blue crosses in Fig. 5. The calculation shows that the expected beam ion current is up to 0.5  $\mu\text{A}$ , which is comparable with the signal level of a FILD in the CHS [4].

Development of the fast-ion loss detector for W7-X is performed by means of LORBIT and ASCOT codes. It is found that barely co-going and trapped particles are expected to be measured by the FILD installed on the MPM. The expected FILD signal will be up to 0.5  $\mu\text{A}$ . The FILD with Faraday film layout pattern (b) will be applied to the W7-X for investigating beam ion losses induced by non-axisymmetric magnetic field ripple as well as MHD instabilities.

#### Acknowledgments

This work is supported by the NINS program of Promoting Research by Networking among Institutions (Grant Number 01411702) and NIFS Stellarator-Heliotron Association. Committee (URSX209). This work has been carried out within the framework of the EUROfusion Consortium and has received funding from the Euratom research and training programme 2014-2018 under grant agreement No 633053. The views and opinions expressed herein do not necessarily reflect those of the European Commission.

#### References

- [1] A. Fasoli *et al.*, Nucl. Fusion **47**, S264 (2007).
- [2] A. Werner *et al.*, *Advanced Diagnostics for Magnetic and Inertial Fusion*, edited by P. E. Stott *et al.* (Kluwer Academic/Plenum, New York, 2002), p. 137.
- [3] D. S. Darrow *et al.*, Rev. Sci. Instrum. **70**, 838 (1999).
- [4] M. Isobe *et al.*, Rev. Sci. Instrum. **77**, 10F508 (2006).
- [5] D. S. Darrow *et al.*, Rev. Sci. Instrum. **72**, 784 (2001).
- [6] F. E. Cecil *et al.*, Rev. Sci. Instrum. **75**, 10 (2004).
- [7] D. S. Darrow *et al.*, Rev. Sci. Instrum. **77**, 10E701 (2006).
- [8] W. P. West *et al.*, J. Nucl. Mater. **337-339**, 420 (2005).
- [9] K. Ogawa *et al.*, Plasma Fusion Res. **8** 2402128 (2013).
- [10] S. Yamamoto *et al.*, Rev. Sci. Instrum. **87** 11D818 (2016).
- [11] M. Isobe *et al.*, J. Plasma and Fusion Res. **8**, 330 (2009).
- [12] N. Rust, Fusion Eng. Des. **86** 728 (2011).
- [13] D. Nicolai *et al.*, Fusion Eng. Des. **123**, 960 (2017).
- [14] E. Hirvijoki *et al.*, Comput. Phys. Commun. **185**, 1310 (2014).
- [15] S. J. Zweben *et al.*, Nucl. Fusion **30**, 1551 (1990).